1. Failure due to perforation in corrugated board boxes

Johan Alfthan, Olof Tillander, Thomas Trost, Aron Tysén, Annika Kihlstedt

Innventia AB
Box 5604, SE-114 86 Stockholm, Sweden

1.1 Abstract

Corrugated board boxes are often used as secondary packaging to protect consumer goods during transport. In shelf ready packaging, the boxes are perforated so that the front and top of the box can be easily removed and the remainder of the box can be used to store and display the goods. The perforations however also make the box weaker and less efficient for protection. The balance between the requirements is today found by trial and error, but could benefit from a more systematic approach. In this study, we started with one of the basic tests of corrugated board boxes, the box compression test. A reference box without perforation and three boxes with different perforation were tested. During the box compression test, a pressure sensitive film registered the distribution of load, an IR camera registered heat from dissipative processes such as plasticity and fracture, and a displacement transducer was used to measure out-of-plane deflection of box panels. All boxes, independent of perforation, failed at similar compression forces, suggesting that the box compression test alone is not an adequate test for performance of the perforated boxes. It was however observed that the perforation did influence the failure of the boxes. The proximity to perforation affected where the panels failed. Analysis of displacement indicated that the perforations mainly were loaded in compression or shear. During transport and handling, more severe loading situations for the perforations would occur which other tests can capture. Vibration tests can be used to study fatigue. Box compression tests with misaligned stacked boxes, loading of the whole box in other modes such as shear, or drop tests will all introduce complex loading were also tension and out-of-plane shear will occur. Climate tests can give effects similar to fatigue. Climate variations also has a large effect on creep.

1.2 Introduction

Corrugated board boxes are used as secondary packaging for many types of consumer goods to protect the goods during transport and handling. Traditionally the secondary packaging is removed at retail but shelf ready packaging (SRP) is an alternative that becomes more common (Levinson 2006). In SRP just the top and front are removed from the box and the remainder is used to store and display the goods. While handling may become more efficient the new designs also provide new challenges. Perforation of the corrugated board is necessary to enable removal of the top and front, but the box should still be able to protect the goods during transport. This engineering problem is solved today by trial and error but design and production could benefit from a more systematic approach. Very little research on the topic has been published. Published articles like Levinson (2006) tend to focus on the market rather than the engineering problems.

In this study, we started with one of the basic tests of corrugated board boxes, the box compression test (BCT). The goal was to identify failure mechanisms, and to accomplish this, the BCT was complemented

with other measurement techniques. Four different box designs were tested, a reference box without perforation (a so called stock keeping unit, SKU), and three perforated boxes (SRP).

1.3 Materials and methods

Four different box designs were investigated, a reference box without perforation denoted SKU Concept A and three boxes with perforation at different positions on the panels denoted SRP Concept A, B and C (Figure 1). All boxes were regular slotted containers, with panel widths of 487 mm and 338 mm and panel height 340 mm. The perforated boxes SRP Concept A, B and C had perforations allowing most of the front panel, the whole top, and a small part of the back panel to be removed when opening the box. In SRP Concept C the front corners of the sides were also removed during opening. The perforated boxes also had holes along the perforations on the front and back panels and at the center of the side panels. The material was an asymmetric 3 mm thick B-flute corrugated board with one white and one brown liner which fulfilled the EUPS 50 specifications (End Use Performance Standard, http://bfsv.de/eups/frameie.html; Table 1). The boxes were manually raised and sealed with adhesive tape.

(a) (b)

Figure 1. The perforated boxes before (a) and after (b) removal of front and top, from left to right SRP Concept A, SRP Concept B and SRP Concept C.

Table 1. Properties of EUPS 50 corrugated board. The values for each property are the average and a guaranteed value based on 95 % confidence level.

Property	Average value	Guaranteed value
Bending stiffness, geometrical mean [Nm]	3.3	3.1
Edge crush test (ECT) [kN/m]	5.4	5.0
Burst strength [kPa]	1000	850
Flat crush test (FCT) [kPa]	380	340

The box compression test (BCT) is a common test of corrugated board container performance, where a single box or a small stack is compressed between two plates from top to bottom. In this study, BCT was carried out according to ASTM D642-00 in standard laboratory climate, 23°C and 50% RH, on single empty boxes at a compression rate of 50 mm/min in a fixed platen testing machine. The whole force-displacement curves were obtained. In addition to BCT, other measurement techniques were utilised, see Figure 2. A pressure sensitive film was used to register the distribution of load during the tests. In each test, one panel of the box was filmed with an IR camera so heat from dissipative processes could be registered. The out-of-plane displacement of this panel was also measured using a displacement transducer positioned in the middle of the panel.

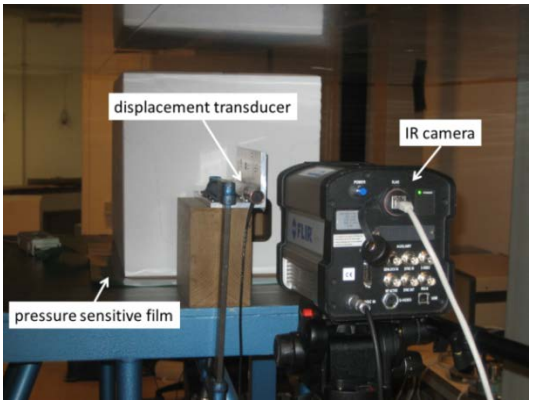

Figure 2. BCT with additional equipment: Pressure sensitive film to register load distribution, IR camera to register heat dissipation and a displacement transducer to measure out-of-plane displacement of the panel.

The I-Scan system from Tekscan Inc. (South Boston, MA, USA; www.tekscan.com) is a pressure measurement system that records real-time static and dynamic pressure data. The I-Scan system is based on a pressure sensitive film. The pressure sensitive film can be used to register the distribution of load during BCT (Meng 2007; Jamialahmadi 2008). The pressure sensitive film used in the tests presented here was the Model 3150, MatScan, with a saturation pressure of 0.689 MPa (100 psi). This model had an array of 2288 (52×44) force sensitive cells called sensels. Each sensel was 70.56 mm^2 (8.4 mm×8.4 mm) in size. The total film area was 432 mm×368 mm. This meant that one short side (front or back) and around 90 % of the long sides could be covered by the film.

The IR camera (FLIR SC6000) was used to film one of the box panels in each test so the heat produced by dissipative processes such as plasticity and fracture could be observed (Hyll et al. 2012). The displacement transducer was a major heat source that had to be avoided during filming with the IR camera. Hence only a part of the panel could be filmed during testing. In most tests the bottom right corner was filmed, since the behaviour of the bottom corners were most influenced by the perforation. A few additional tests were made where the displacement transducer was removed and the whole panel was filmed. The IR camera was not calibrated specifically to the material so the heat signal registered could not be used to calculate exact temperatures or dissipated energies.

The out-of-plane displacement of one of the panels was measured using a displacement transducer (RDP Electronics DCT1000A, using Contrec AQ-Box and Contrec Winlog 2000 for data collection) positioned in the middle of the panel. The out-of-plane displacement and the BCT displacement were used to estimate the deformations and strain state of the panel.

Both in-plane and out-of-plane displacements of the panel contributed to the strain state. The strain depended on the position, both in-plane position given by coordinate x in the horizontal direction of the panel and coordinate y in the vertical direction, and the position in the thickness direction of the panel, which was given by coordinate z. The in-plane displacements were given by the two components u and v in the x and y directions. For simplicity it was assumed that the only in-plane displacements during BCT was the compression v_0, which then gave the in-plane components as

$$u = 0, \tag{1}$$

$$v = -\frac{v_0 y}{H}, \tag{2}$$

where H is the height of the panel.

The out-of-plane displacement w depended on the position on the panel. In this study the displacements were only measured in the middle of the panel, so an assumption had to be made for the displacements elsewhere. For simplicity it was assumed that the panel buckled symmetrically into a double curved shape. For the analysis, this shape was further assumed to be given by the equation

$$w = w_0 \sin\left(\frac{\pi x}{W}\right)\sin\left(\frac{\pi y}{H}\right), \tag{3}$$

where w_0 is the measured displacement at the middle of the panel, W the width and H the height of the panel.

From the displacements, normal strains ε_x and ε_y and shear γ_{xy} could be calculated using plate theory from solid mechanics. The out-of-plane displacement was so large that the stretching of the panel had to be taken into account. The non-linear von Karman plate theory (see e.g. Fung 1965) was hence adopted. According to this theory, the strains were given by the equations

$$\varepsilon_x = \frac{\partial u}{\partial x} - z\frac{\partial^2 w}{\partial x^2} + \frac{1}{2}\left(\frac{\partial w}{\partial x}\right)^2, \tag{4}$$

$$\varepsilon_y = \frac{\partial v}{\partial y} - z\frac{\partial^2 w}{\partial y^2} + \frac{1}{2}\left(\frac{\partial w}{\partial y}\right)^2, \tag{5}$$

$$\gamma_{xy} = \frac{\partial u}{\partial y} + \frac{\partial v}{\partial x} - 2z\frac{\partial^2 w}{\partial x \partial y} + \frac{\partial w}{\partial x}\frac{\partial w}{\partial y}, \tag{6}$$

where the stretching was taken into account by the last term in each equation. The normal strain ε and shear γ acting on the perforation were calculated, using the equations

$$\varepsilon(\varphi) = \varepsilon_x \cos^2(\varphi) + \varepsilon_y \sin^2(\varphi) + \gamma_{xy}\cos(\varphi)\sin(\varphi), \tag{7}$$

$$\gamma(\varphi) = (\varepsilon_y - \varepsilon_x)\sin(2\varphi) + \gamma_{xy}\cos(2\varphi), \tag{8}$$

where φ is an angle denoting the normal direction of the perforation according to Figure 3.

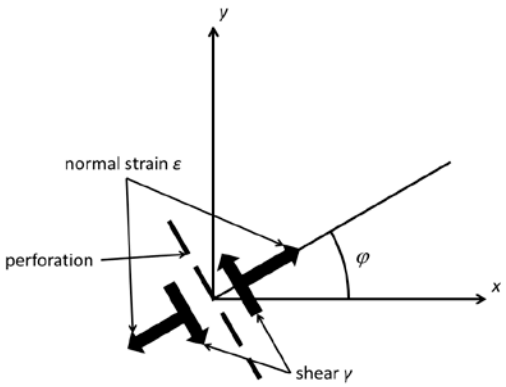

Figure 3. Definition of positive normal strain ε and positive shear γ along a perforation with normal in the φ direction.

1.4 Results

The results of the BCT testing are summarised in Table 2. On the front of the perforated boxes, failure of corners occurred close to the perforations and the buckling shape was determined by the perforated lines, which were more compliant than the rest of the panels and hence easily folded. Boxes with different types of damages after BCT are shown in Figure 4. The force and out-of-plane displacement as function of BCT

displacement are shown in Figures 5–8. The perforated front panels tended to buckled outwards, at least initially during the BCT testing, while the back panels of the perforatated boxes tended to buckle inwards.

Table 2. Results of the BCT testing of the four different box designs. The mean BCT strength and BCT displacement at failure are shown with 95% confidence intervals.

Box design	Number of tests	BCT strength [kN]	BCT displacement at failure [mm]
SKU Concept A	7	2.448±0.201	7.54±0.76
SRP Concept A	5	2.238±0.165	8.18±1.01
SRP Concept B	6	2.248±0.151	7.83±1.12
SRP Concept C	8	2.348±0.141	7.28±0.84

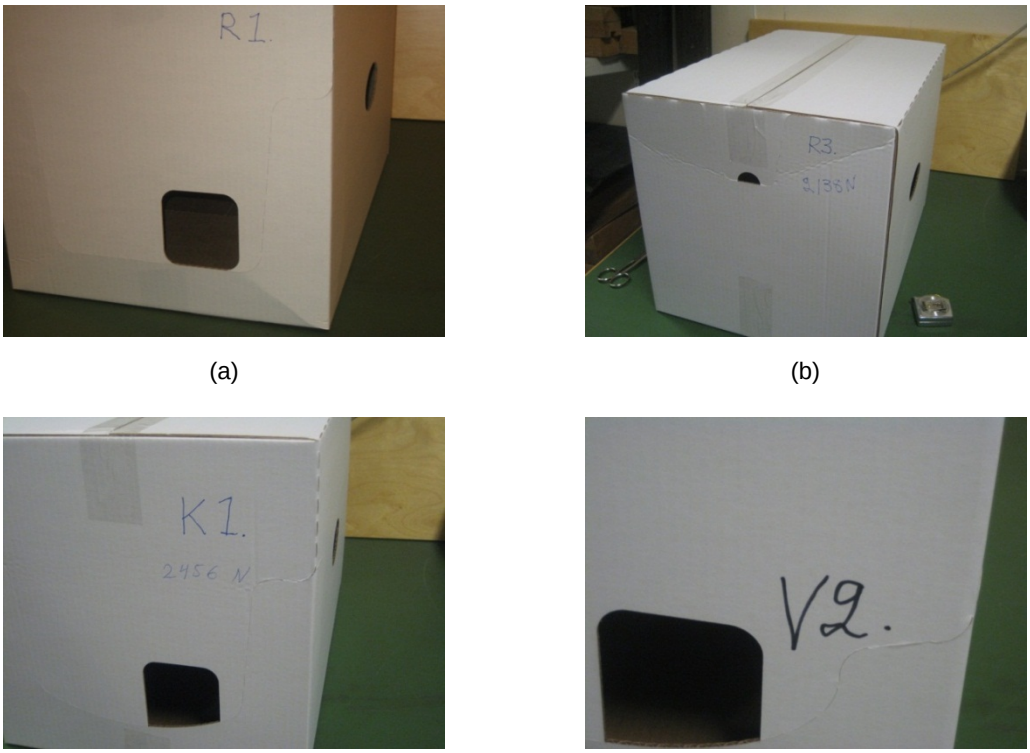

(a) (b)

(c) (d)

Figure 4. Examples of different types of damages after BCT: (a) SRP Concept A, failure of bottom corners of the front panel going from the corners to the perforation; (b) SRP Concept A, failure of top corners of the back panel going from the corners to the perforation; (c) SRP Concept B, failure of perforation halfway up on front panel; (d) SRP Concept C, failure of perforation halfway up on front panel.

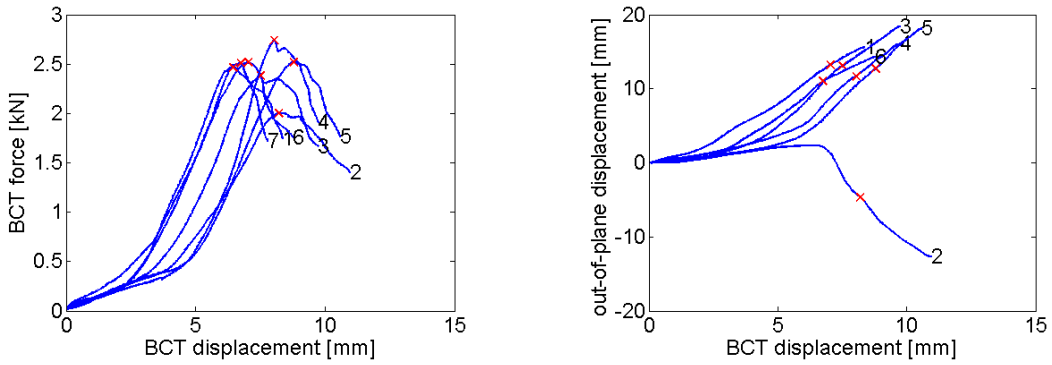

(a) (b)

Figure 5. Results for reference box SKU Concept A: (a) BCT force-displacement curves; (b) out-of-plane displacement as function of BCT displacement. The crosses mark failure and the numbers denote different tests. Negative out-of-plane displacement means that the panel buckled inwards.

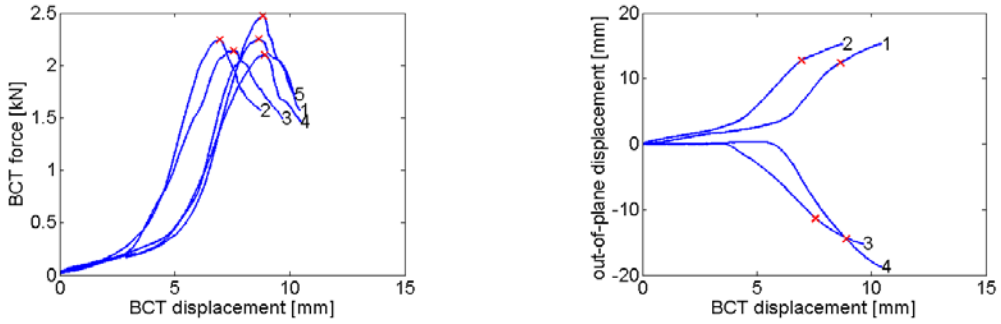

(a) (b)

Figure 6. Results for SRP Concept A: (a) BCT force-displacement curves; (b) out-of-plane displacement as function of BCT displacement. The crosses mark failure and the numbers denote different tests. For test number 1 and 2 the out-of-plane displacement was measured on front panels and for test number 3 and 4 on back panels. Negative out-of-plane displacement means that the panel buckled inwards.

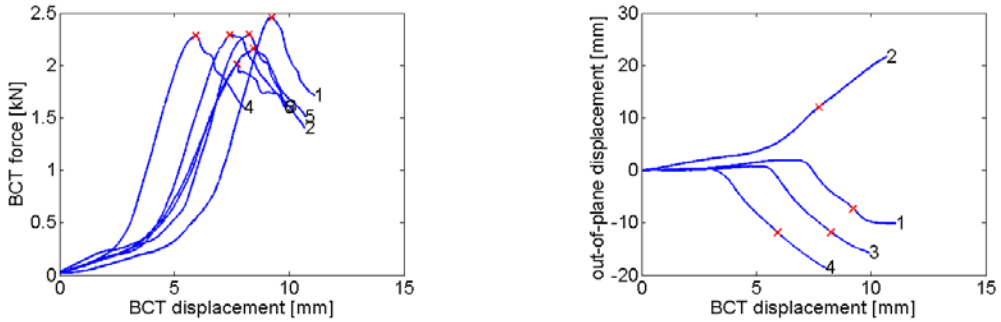

(a) (b)

Figure 7. Results for SRP Concept B: (a) BCT force-displacement curves; (b) out-of-plane displacement as function of BCT displacement. The crosses mark failure and the numbers denote different tests. For test number 1 and 2 the out-of-plane displacement was measured on front panels and for test number 3 and 4 on back panels. Negative out-of-plane displacement means that the panel buckled inwards.

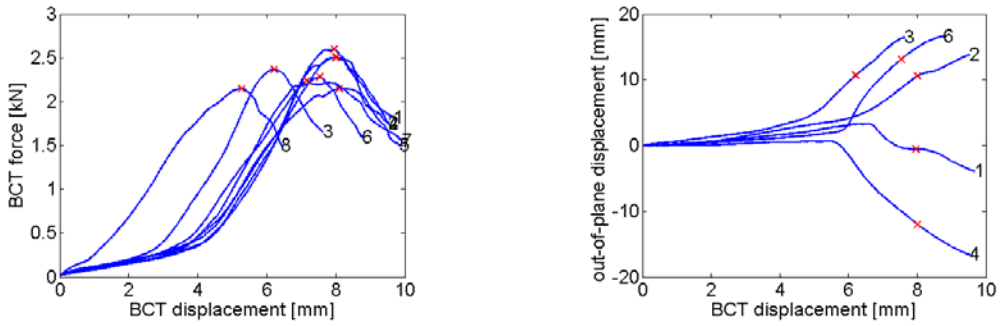

(a) (b)

Figure 8. Results for SRP Concept C: (a) BCT force-displacement curves; (b) out-of-plane displacement as function of BCT displacement. The crosses mark failure and the numbers denote different tests. For test number 1, 2 and 3 the out-of-plane displacement was measured on front panels and for test number 4 and 6 on back panels. Negative out-of-plane displacement means that the panel buckled inwards.

The pressure sensitive film gave the force distribution on the box edges during BCT. Examples are shown in Figure 9. Since the boxes were empty only the edges and corners took up load. The highest forces were found near the corners. At failure the front panel was often unloaded when it buckled. No large differences between the different box designs could be observed. The details of the force distributions were hard to interpret. Small differences between the boxes, probably mainly from folding and sealing of the top and bottom, had an effect on the distributions.

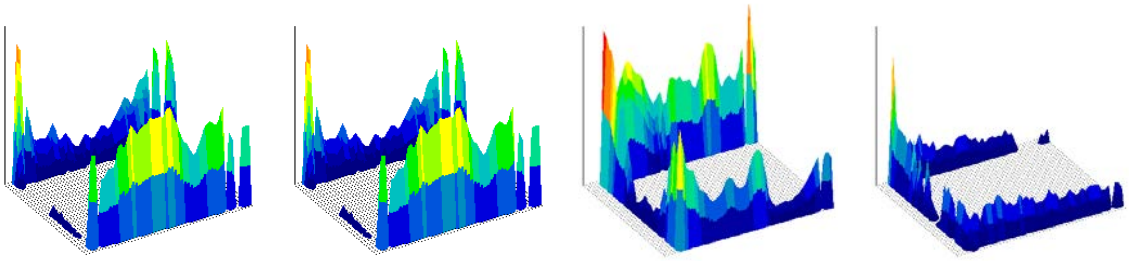

(a) (b) (c) (d)

Figure 9. Examples of force distribution on the front panel of the different boxes designs at failure: (a) the reference box SKU Concept A; (b) SRP Concept A; (c) SRP Concept B,; (d) SRP Concept C.

With the IR camera, heat produced by plastic deformations and damages was registered. The IR camera did not always capture a failure zone since it was difficult to predict where plasticity and damages would occur. Selected results are shown in Figure 10. Hot areas were damage occurred is in light colours and cold areas in dark colours. For the reference box SKU Concept A damages in the corners were observed but did not always occur in all corners at the same time. For SRP Concept A, damages regularly occurred at the bottom corners but also along the perforation on the front panel. For SRP Concept B, damages occurred at the bottom corners but could also occur at the horizontal perforation halfway up on the front. For SRP Concept C the damages often occurred at the horizontal perforation halfway up on the front. The diagonal perforated line on the sides of SRP Concept C seldom failed, but might have had an influence on other damages.

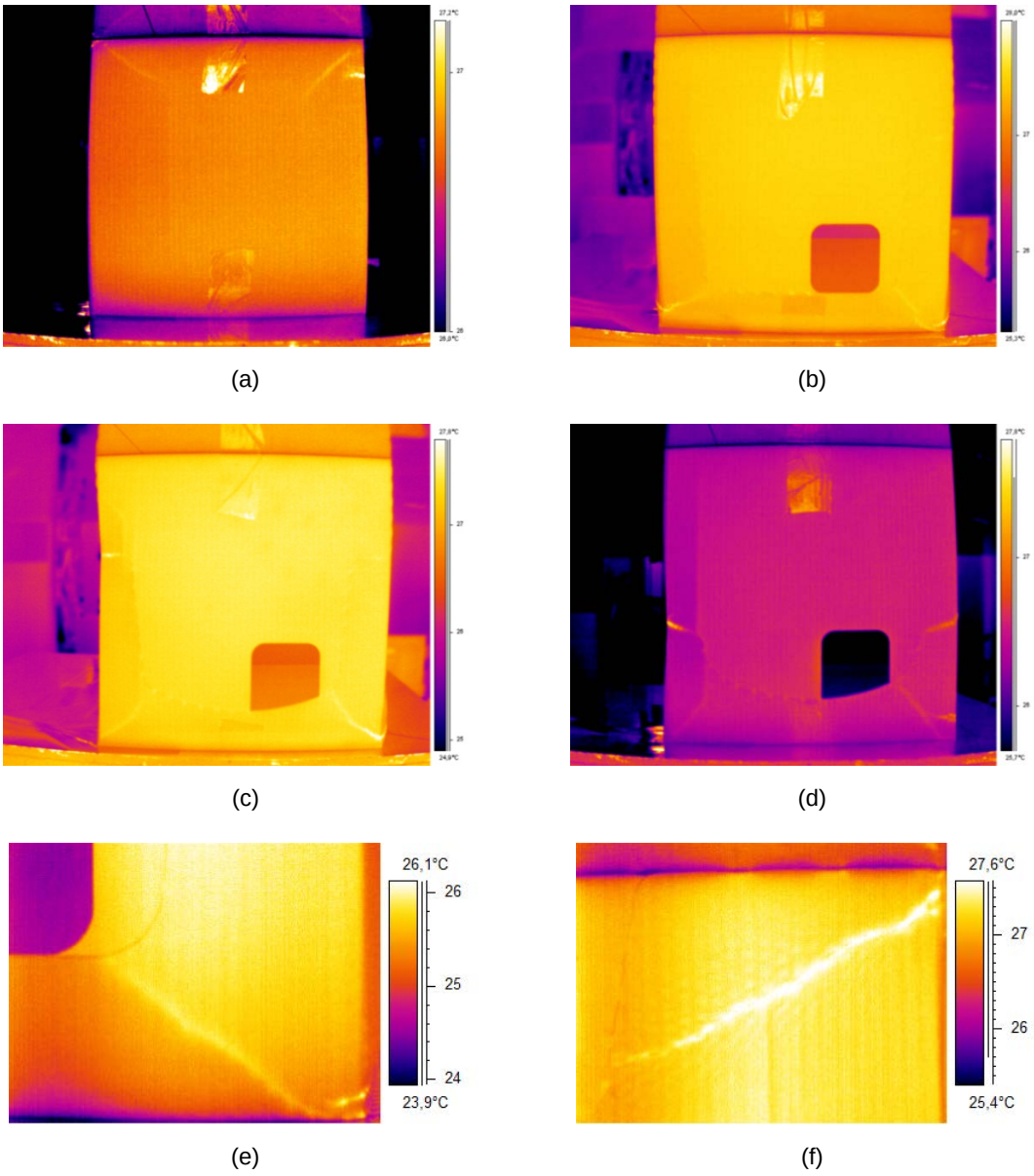

Figure 10. Examples of failure of the different box designs captured with the IR camera: (a) front panel of reference box SKU Concept A; (b) front panel of SRP Concept A; (c) front panel of SRP Concept B; (d) front panel of SRP Concept C; (e) bottom right corner of front panel of SRP Concept A; (f) top right corner of back panel of SRP Concept A.

The strain state was calculated according to Eqs (4–6) and the projected normal strain and shear along the perforation were calculated according to Eqs (7–8). In Figures 11–13, the normal strains and shear on the perforation of the front panel at peak BCT force are shown for one test from each type of box where the panel buckled outwards. The out-of-plane coordinate z was set to half the thickness, which corresponded to the outer surface of the corrugated board panel that was observed. The strain state was dominated by the strain component ε_y, which was mainly determined by the compressive displacement in BCT. The strains on horizontal perforation were compressive while much smaller tensile strains occur on vertical perforation. The shear varied along the perforation but was mostly negative on the left side of the panel and positive on the right following the definition in Figure 3. SRP Concept B and C, with the curved middle section of the perforation had less compressive strain and higher shear along that section compared to SRP Concept A with a straight middle section. Peaks in shear occurred at the radii connecting line seg-

ments along the perforation, which was a result of the domination strain component ε_y, which projected in 45° corresponded to shear.

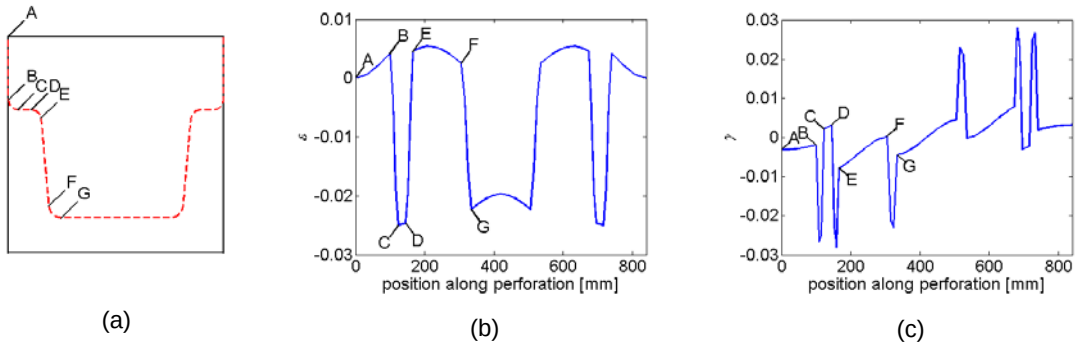

Figure 11. Strain on perforation on the front panel of SRP Concept A: (a) path followed to calculate strain and shear on the perforation; (b) normal strain ε on perforation; (c) shear γ on perforation.

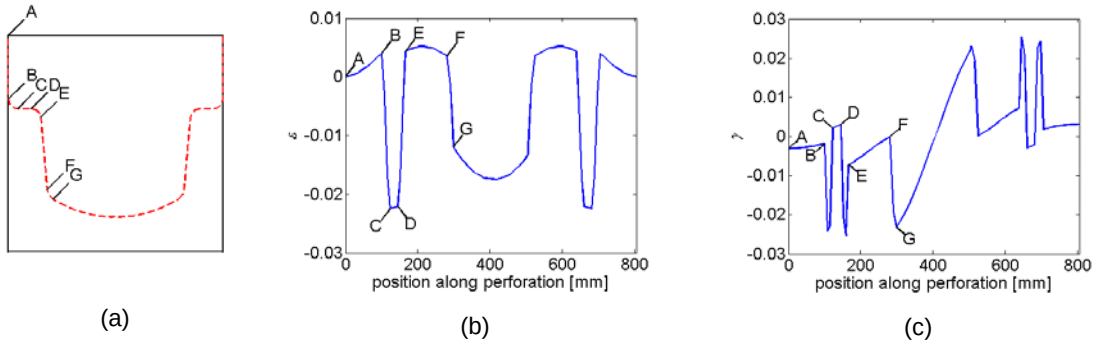

Figure 12. Strain on perforation on the front panel of SRP Concept B: (a) path followed to calculate strain and shear on the perforation; (b) normal strain ε on perforation; (c) shear γ on perforation.

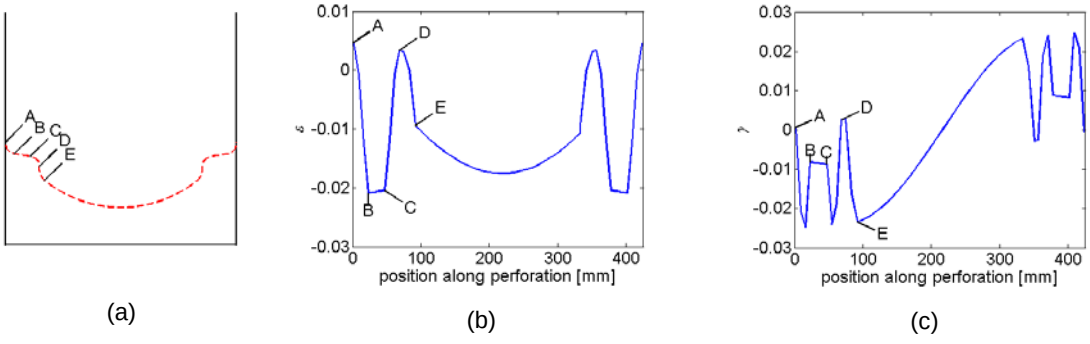

Figure 13. Strain on perforation on the front panel of SRP Concept C: (a) path followed to calculate strain and shear on the perforation; (b) normal strain ε on perforation; (c) shear γ on perforation.

1.5 Discussion

In BCT, all boxes independent of perforation failed at similar compression forces, suggesting that BCT alone is not an adequate test for performance of the perforated boxes. The force distribution during BCT was also similar on the different box types. The perforation did however influence the failure of the boxes. The front of the box which had most of the perforation tended to buckle outwards at least initially, while the back tended to buckle inwards. The perforated lines were more compliant than the rest of the panel and folded during buckling. Dissipative processes, likely both plastic deformations and fracture, could be observed along those lines. The bottom corners of the front panel failed due to the proximity to perforation. In some cases the front panel for SRP Concept B and C failed at the perforation halfway up on the front. The holes on the sides of the boxes did not seem to affect failure.

Analysis of the out-of-plane displacement indicated that the perforations mainly were loaded in compression or shear. For SRP Concept B and C the highest compressive strains occurred at the perforation halfway up on the front, which might explain why these boxes often failed there. The compressive loading of the perforation meant that even though the perforations were damaged, forces could be transferred through the contact of fracture surfaces resting on each other. This might explain the small differences in BCT strength between the different box types.

The findings in this study do not capture empirically observed differences in performance for different designs. The loading is more complex than BCT loading during normal use of the box, e.g. during transport. The load directions are likely to be different from BCT. Loading may also vary with time. This can be short term variations such as vibrations and impact, and long term variations over the box lifetime such as stacking and handling as well as climate induced loading. This might lead to tensile or out-of-plane shear loading of the perforation which are more likely to cause failure. Fatigue, i.e. cyclic loading of the material, might also lead to a degradation of the perforation which could not be observed in BCT.

Several tests are of interest to build better knowledge on the performance of perforated boxes. Vibration testing of perforated single or stacked boxes could be performed to study fatigue. These tests could be interrupted for other testing, e.g. BCT, to study the degradation.

BCT can also be performed on stacks of boxes. In the stacks the individual boxes might be loaded differently from the single box BCT, which might lead to more severe loading of the perforations and thus worse box performance in BCT. The whole box can also be loaded in different modes such as shear. A box could e.g. be mounted diagonally in the box compression test so that diagonal edges carry the load to introduce shear in the box panels. This would result in tension on some of the perforations. The effect of the complex loading occurring during sudden impact can be studied in drop tests.

Climate influences material properties and it can thus also influence the performance of the perforated box. This effect could be similar to fatigue and could thus be studied in a similar way by interrupting the test for other testing. Especially at high or varying humidity, creep will be important if forces are also applied to the box. Depending on loading direction the effect on perforation might be large.

1.6 Conclusions

BCT was not directly affected by perforation, so BCT alone is not an adequate test for performance of the perforated boxes.

The damages occurring in the box during BCT were however affected by perforation. The proximity to perforation influenced how corner failures developed and in some cases the failure occurred directly in the perforation.

The perforation of the boxes were mainly loaded in compression or shear. This kind of loading might be less severe than situations occurring during handling and transport.

To summarise, the compressive force and displacement levels at failure in BCT were not affected by perforations, but when damage occurred it was to an extent following the perforations.

References

Fung Y C (1965), *Foundations of solid mechanics*, Prentice-Hall, Inc., Eaglewood Cliffs, USA

Hyll C, Vomhoff H, Nygårds M (2012), *Analysis of the visco-plastic and elastic energy during the deformation and rupture of a paper sample using thermography*, Paper Physics Conference 2012, Stockholm

Jamialahmadi A (2008), *Experimental and numerical analysis of the dynamic load distribution in a corrugated packaging system*, MSc thesis, KTH

Levinson M (2006), *Off the shelf: the inexorable growth of retail ready packaging*, Packaging September 2006, 12-16

Meng G (2007), *Experimental and numerical analysis of the load distribution in a corrugated packaging system*, MSc thesis, KTH